Rate-equation model for quantitative concentration measurements in flames with picosecond pump–probe absorption spectroscopy

Gregory J. Fiechtner, Galen B. King, and Normand M. Laurendeau

Measurement of radical concentrations is important in understanding the chemical kinetics involved in combustion. Application of optical techniques allows for the nonintrusive determination of specific radical concentrations. One of the most challenging problems for investigators is to obtain flame data that are independent of the collisional environment. We seek to obviate this difficulty by the use of picosecond pump–probe absorption spectroscopy. A picosecond pump–probe absorption model is developed by rate-equation analysis. Implications are discussed for a laser-pulse width that is much smaller than the excited-state lifetime of the absorbing atom or molecule. The possibility of quantitative, quenching-independent concentration measurements is discussed, and detection limits for atomic sodium and the hydroxyl radical are estimated. For a three-level absorber–emitter, the model leads to a novel pump–probe strategy, called dual-beam asynchronous optical sampling, that can be used to obtain both the electronic quenching-rate coefficient and the doublet mixing-rate coefficient during a single measurement. We discuss the successful demonstration of the technique in a companion paper [Appl. Opt. **34,** XXX (1995)].

Key words: Combustion, sodium, picosecond phenomena, absorption, spectroscopy.

1. Introduction

Optical methods of measuring species concentrations have provided new insights into the combustion process.[1] The most widely used of these techniques is laser-induced fluorescence,[2] because its favorable signal-to-noise ratio permits detection of minor species such as the hydroxyl radical. However, fluctuations in the collisional environment can cause uncertainty in the laser-induced fluorescence signal.[3] To overcome this difficulty, we have previously examined the possibility of using synchronously mode-locked dye lasers with picosecond pulses in the pump–probe configuration. These techniques will potentially allow us to measure minor species concentrations that are independent of the collisional environment. In particular the asynchronous optical sampling (ASOPS) technique has been applied to atomic sodium in laminar flames at atmospheric pressure.[3]

We present a model that permits quantitative concentration measurements by the use of picosecond pump–probe absorption spectroscopy. The model is based on the standard rate equations for a small laser irradiance. This approach is often questioned when the laser-pulse width is much smaller than the inverse of the electronic quenching-rate coefficient.[4] Nevertheless we have successfully applied the rate equations under these conditions. Using the detection limit for atomic lithium reported by Jones and coworkers,[5] we predict detection limits for atomic sodium and the hydroxyl radical The model is extended to measurements of excited-state lifetimes, resulting in a novel procedure for obtaining electronic quenching-rate coefficients for a multilevel absorber–emitter. Quantitative experimental results for atomic sodium are presented in a companion paper, which also summarizes the significant features of the ASOPS method.[6]

2. Overview

The rate-equation model is introduced in Section 3. Solutions to the rate equations are also considered in Section 3, and specific expressions for a synchronously mode-locked dye laser are included in Section

When this research was performed the authors were with the Flame Diagnostics Laboratory, School of Mechanical Engineering, Purdue University, West Lafayette, Indiana 47907. G. J. Fiechtner is now with the Combustion Research Facility, Sandia National Laboratories, Livermore, California 94551.

Received 6 October 1993; revised manuscript received 27 June 1994.

0003-6935/95/061108-09$06.00/0.

4. The maximum operating power so as to avoid optical saturation and the concentration that corresponds to the limit of optical thickness are calculated in Sections 5 and 6, respectively. The model is extended to include absorption in the pump–probe configuration in Section 7. Close agreement with experimental values obtained in previous investigations is found. The delay between a pump pulse and a probe pulse is considered in Section 8, so that the measurement of excited-state lifetimes can be modeled. In Section 9 the model is used to describe a new measurement technique, which we call dual-beam ASOPS. Finally, the absence of coherent transient effects is considered in Section 10.

3. Rate-Equation Method

Consider the two-level absorber–emitter shown in Fig. 1(a). The pump laser is tuned to resonance with the 1–2 transition, and the probe laser is tuned to resonance with either the 1–2 or the 2–3 transition. An additional intermediate energy level is often necessary; for example, our previous measurements require that we use two intermediate states to model the $3P_{1/2,3/2}$ doublet of atomic sodium adequately.[3] To demonstrate the difficulties that can arise in this situation, we also consider the three-level absorber–emitter shown in Fig. 1(b). For the three-level absorber–emitter the pump laser can be tuned to either the 1–2 or the 1–3 transition, and the probe laser can be tuned to the 1–2, 1–3, 2–4, or 3–4 transition. The number density of the ith level in Fig. 1 is denoted by N_i [in inverse cubic centimeters (cm^{-3})], and the total number density, N_T (cm^{-3}) is the sum of the number densities over all the levels of a particular model.

We now define a number of processes associated with the models shown in Fig. 1. The laser interacts with the absorber–emitter through W_{ij} and W_{ji}, which represent the rate coefficients for stimulated absorption and stimulated emission [in inverse seconds (s^{-1})] between levels i and j, respectively. The Einstein rate coefficient is A_{ji} (s^{-1}) for spontaneous emission and B_{ij} [in cubic centimeters times frequency per Joule times seconds ($\mathrm{cm}^3\ \mathrm{s}^{-1}/\mathrm{Js}$)] for stimulated absorption. Population transfer is also permitted to take place as a result of collisions. Thus Q_{ji} represents the collisional deexcitation rate coefficient, often called the quenching-rate coefficient (s^{-1}). Because the transitions in question occur in the visible or the UV regions of the spectrum, collisional excitation is negligible relative to quenching.[7] For the same reason the excited-state population is negligible in the absence of laser irradiation, so that N_T is approximately equal to N_1. In Fig. 1(b), Q_{23} and Q_{32} represent the mixing-rate coefficients (s^{-1}) between levels 2 and 3.

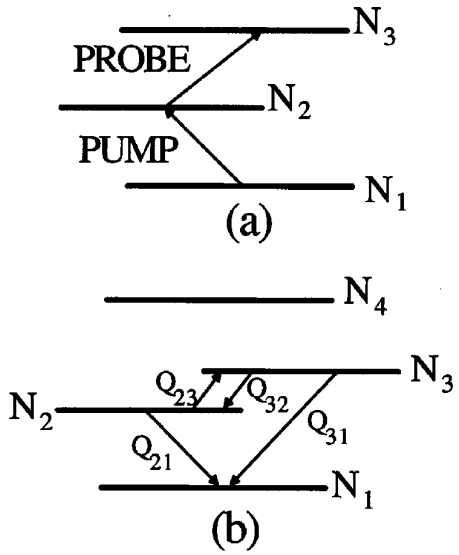

Fig. 1. Pump–probe diagrams corresponding to (a) a two-level absorber–emitter and (b) a three-level absorber–emitter. In both cases one level is added to account for the probe, resulting in a total of (a) three and (b) four levels.

Two-Level Absorber

The excited-state number density can be related to the total number density with the rate equation for a two-level atom[2]:

$$\frac{\mathrm{d}N_2}{\mathrm{d}t} = N_T W_{12} - N_2\left[\left(1 + \frac{g_1}{g_2}\right)W_{12} + T_{21}\right]. \tag{1}$$

In Eq. (1) the stimulated Einstein rate coefficients can be written as[8]

$$W_{12} = \frac{g_2}{g_1} W_{21} = \frac{B_{12}}{c}\int_{-\infty}^{\infty} I_\nu^L Y(\nu)\,\mathrm{d}\nu, \tag{2}$$

where I_ν^L is the laser spectral irradiance ($\mathrm{W/cm}^2\ \mathrm{s}^{-1}$), $Y(\nu)$ is the spectral line-shape function [expressed in seconds (s)] for the resonant transition, g_i represents the degeneracy of the ith state, and $T_{ji} = Q_{ji} + A_{ji}$. By applying the appropriate spectral and temporal approximations, we can express W_{12} in terms of the average laser power, as shown in Section 4.

A number of situations arise in which the time-dependent nature of Eq. (1) can be ignored. At steady state, $\mathrm{d}N_2/\mathrm{d}t = 0$, and Eq. (1) yields

$$(N_2)_{\mathrm{ss}} = \frac{N_T W_{12}}{\left(1 + \frac{g_1}{g_2}\right)W_{12} + T_{21}}. \tag{3}$$

Equation (3) will apply (a) for cw laser excitation or (b) at the peak of a laser pulse with a temporal width that is sufficiently large compared with the lifetime of level 2.[2] For small laser irradiance, $W_{12} \ll T_{21}$, whereas for large laser irradiance, $W_{12} \gg T_{21}$, so that

$$(N_2)_{\mathrm{SS}}{}^{\mathrm{LIN}} = \frac{N_T W_{12}}{T_{21}}, \tag{3a}$$

$$(N_2)_{\mathrm{SS}}{}^{\mathrm{SAT}} = \frac{N_T g_2}{g_1 + g_2}, \tag{3b}$$

in the linear and the saturated limits, respectively.

The time-dependent solution to Eq. (1) is given by[4]

$$N_2^*(t) = \frac{(N_2)_{SS}}{N_T}\{1 - \exp[-(W_{12} + W_{21} + T_{21})t]\}, \quad (4)$$

where we have assumed that the laser pulse has a temporal top-hat profile and defined the dimensionless population density of the ith level as $N_i^* = N_i/N_T$.

B. Three-Level Absorber

Models for sodium and other alkalis require an additional level because of spectroscopic doublets. For the three-level absorber, level 1 is again the ground level, and levels 2 and 3 are reserved for the doublet levels. The first-order exponential of Eq. (4) no longer applies because two first-order rate equations must be solved simultaneously. Because of the presence of the additional level, we introduce the rate coefficients W_{13}, W_{31}, and T_{31}, along with the doublet mixing-rate coefficients Q_{23} and Q_{32}.

The transient solution of the three-level rate equations has been extensively reported.[4] The results are summarized here so that the appropriate expressions can be used in the pump–probe model. Because obtaining the solution in terms of the original rate coefficients would be cumbersome, we consider the direct application of the rate equations to atomic sodium.[3,6] Let 1, 2, and 3 denote the $3S_{1/2}$, $3P_{1/2}$, and $3P_{3/2}$ states, respectively. Because only 0.6 nm separates the D_1 and D_2 transitions, we may assume[7] that $Q_{21} = Q_{31} = Q$. In addition, for sodium $A_{21} = A_{31} = A$. By relating levels 2 and 3 through the principle of detailed balancing, we can show that $Q_{23} = 2Q_{32}$ at flame temperatures.[7] The dimensionless number densities of the excited doublet after laser irradiation are then[9,10]

$$N_2^*(t) = 1/3\{(N_{3,0}^* + N_{2,0}^*)\exp[-(Q + A)t] - (N_{3,0}^* - 2N_{2,0}^*)\exp[-(Q + A + 3Q_{32})t]\}, \quad (5)$$

$$N_3^*(t) = 2/3\{(N_{3,0}^* + N_{2,0}^*)\exp[-(Q + A)t] + (1/2N_{3,0}^* - N_{2,0}^*)\exp[-(Q + A + 3Q_{32})t]\}. \quad (6)$$

In Eqs. (5) and (6) $N_{2,0}^*$ and $N_{3,0}^*$ are the initial dimensionless excited-state population densities for 1–2 and 1–3 excitation, respectively, which vanish in the absence of laser irradiation. These expressions are used in Section 9 to develop a model for general temporal pump–probe spectroscopy that is applicable to results such as those obtained when the ASOPS instrument is used for measurement of atomic sodium.[3,6]

4. Synchronously Mode-Locked Laser Radiation

Before continuing with the present rate-equation analysis, we must express the stimulated absorption rate coefficient W_{12} in terms of practical experimental parameters. The evaluation of W_{12} requires the application of both spectral and temporal approximations concerning the output of a synchronously mode-locked dye laser.

The spectral bandwidth (FWHM) $\Delta\nu_{1/2}{}^L$ (s^{-1}) can be estimated from the laser-pulse width, which can easily be measured with second-harmonic autocorrelation. The spectral line shape is related to the autocorrelation pulse shape because the output pulses are nearly Fourier-transform limited. In this case $\Delta\nu_{1/2}{}^L\Delta t_{1/2}{}^L$ is a constant, where $\Delta t_{1/2}{}^L$ (s) is the temporal pulse width (FWHM). Blanchard and Wirth[11] have shown that the spectral distribution of a pulse is best modeled with a sech^2 function that results in a time–bandwidth product of 0.32. Choosing this function, we can write the spectral line-shape function of the laser as[10]

$$Y^L(\nu) = \frac{\ln\left(\frac{1}{\sqrt{2}-1}\right)}{\Delta\nu_{1/2}{}^L}\,\mathrm{sech}^2\left[\frac{2\ln\left(\frac{1}{\sqrt{2}-1}\right)}{\Delta\nu_{1/2}{}^L}(\nu - \nu_0{}^L)\right], \quad (7)$$

where $\nu_0{}^L$ is the central laser frequency (s^{-1}).

The rate equations are usually expressed in terms of the absorption rate coefficient W_{12}, which is given by Eq. (2). A typical pulse width for our laser system is 20 ps,[6] for which the time–bandwidth product yields the value $\Delta\nu_{1/2}{}^L = 1.6 \times 10^{10}\ s^{-1}$. This is much larger than the sodium linewidth[6] of $\Delta\nu_{1/2} = 2.7 \times 10^9\ s^{-1}$, so that $\Delta\nu_{1/2}{}^L \gg \Delta\nu_{1/2}$. In this case, we can evaluate Eq. (2) with $I_\nu{}^L = I^L Y^L(\nu)$ by holding the laser spectral irradiance constant at its centerline value and removing it from the integral.[8] Hence the stimulated rate coefficient and the laser irradiance are related by[10]

$$W_{12} = \frac{B_{12}\ln\left(\frac{1}{\sqrt{2}-1}\right)}{c\Delta\nu_{1/2}{}^L} I^L = \frac{g_2}{g_1}\frac{c^2 A_{21}\ln\left(\frac{1}{\sqrt{2}-1}\right)}{8\pi h\nu_0{}^3\Delta\nu_{1/2}{}^L} I^L, \quad (8)$$

where I^L is the total laser irradiance [in watts per square centimeter (W/cm^2)] and ν_0 is the central transition frequency (s^{-1}).

From an experimental standpoint, the total laser irradiance is not a practical quantity, because average laser power $P_{AVE}{}^L$ (W) is usually measured. To simplify the mathematical modeling of the interaction of laser radiation with an atomic species, each mode-locked laser pulse can be temporally modeled as a top-hat profile. In this case[10]

$$I^L = \frac{P_{AVE}{}^L}{A_c\Delta t_{1/2}{}^L f^L}, \quad (9)$$

where $A_c = \pi D^2/4$ is the cross-sectional area of the laser beam (cm^2), D is the focal diameter (cm) if we assume the cylindrical beam shown in Fig. 2(a), and f^L is the laser repetition frequency (~82 MHz for our

lasers[6]). Combining Eqs. (8) and (9), we can write

$$W_{12} = \frac{g_2}{g_1} \frac{c^2 A_{21} \ln\left(\frac{1}{\sqrt{2}-1}\right) P_{\mathrm{AVE}}{}^L}{2\pi^2 D^2 h \nu_0{}^3 \Delta\nu_{1/2}{}^L \Delta t_{1/2}{}^L f^L}. \tag{10}$$

Equation (10) can also be expressed in terms of the energy per pulse (in joules), $E_p{}^L$, by application of the relation $P_{\mathrm{AVE}}{}^L = f^L E_p{}^L$.

5. Short-Pulse-Width Effects on Saturation

The ASOPS experiments for which this model has been developed require that one have a knowledge of the extent of the linear range with power. A good estimate for the onset of saturation is the saturation parameter, which can be defined as the absorption rate coefficient for which the linear and the saturated solutions to the rate equations are equivalent.[4,10] For the two-level model at steady state, one can obtain the saturation parameter by equating Eqs. (3a) and (3b),[2,4,10]

$$(W_{12})_{\mathrm{SS}}{}^{\mathrm{SAT}} = \frac{T_{21} g_2}{g_1 + g_2}. \tag{11}$$

For the sodium parameters given in part (a) of Table 1, the resulting steady-state saturation parameter becomes $(W_{12})_{\mathrm{SS}}{}^{\mathrm{SAT}} = 1.4 \times 10^9\ \mathrm{s}^{-1}$, which from Eq. (10) corresponds to an average laser power of only $(P_{\mathrm{AVE}}{}^L)_{\mathrm{SS}}{}^{\mathrm{SAT}} = 34\ \mu\mathrm{W}$. For the latter calculation, we have used the laser parameters given in part (b) of Table 1. These parameter values are used for all relevant calculations throughout this paper, unless otherwise noted.

Table 1. Parameters Used in Calculations

(a) Spectroscopic and collisional parameters for the D_2 line of atomic sodium[a]	
Transition 1–2	$3S_{1/2}$–$3P_{3/2}$
ν_0	$5.0934 \times 10^{14}\ \mathrm{s}^{-1}$
A_{21}	$6.15 \times 10^7\ \mathrm{s}^{-1}$
Q_{21}	$2 \times 10^9\ \mathrm{s}^{-1}$
(b) Laser parameters for a synchronously mode-locked dye laser, for which the time–bandwidth product is assumed to be 0.32[b]	
$\Delta t_{1/2}{}^L$	20×10^{-12} s
$\Delta\nu_{1/2}{}^L$	$1.6 \times 10^{10}\ \mathrm{s}^{-1}$
$(\Delta\nu_{1/2})_c$	$2.7 \times 10^9\ \mathrm{s}^{-1}$
f^L	$82 \times 10^6\ \mathrm{s}^{-1}$
D	7.6×10^{-3} cm
Crossing angle	2.9°
(c) Spectroscopic parameters for a particular pump–probe configuration of atomic sodium[a]	
Transition 1–2	$3S_{1/2}$–$3P_{1/2}$ (D_1 line, nonresonant)
Transition 1–3	$3S_{1/2}$–$3P_{3/2}$ (D_2 line, pump)
Transition 3–4	$3P_{3/2}$–$4D_{5/2}$ (probe)
ν_{13}	$5.0934 \times 10^{14}\ \mathrm{s}^{-1}$
ν_{34}	$5.2741 \times 10^{14}\ \mathrm{s}^{-1}$
A_{31}	$6.15 \times 10^7\ \mathrm{s}^{-1}$
A_{43}	$1.23 \times 10^7\ \mathrm{s}^{-1}$

[a]Ref. 10.
[b]Ref. 11.

Previous experiments concerning the onset of saturation with mode-locked lasers for atomic sodium in atmospheric-pressure flames resulted in a much higher value of the saturation parameter.[12] This discrepancy arises, in part, because true steady-state conditions are not achieved for the small pulse widths $\Delta t_{1/2}{}^L$ that are characteristic of mode-locked lasers.[13,14] For a two-level model, the appropriate transient solution is Eq. (4) with $t = \Delta t_{1/2}{}^L$.[4,13] For $W_{12} \ll T_{21}$, we may expand the exponential term by assuming that $\Delta t_{1/2}{}^L$ is small to obtain the linear limit[10,14]

$$(N_2)^{\mathrm{LIN}} = N_T W_{12} \Delta t_{1/2}{}^L. \tag{12}$$

Thus the increase in excited-state population is directly proportional to both the incident laser power and the pulse width. For $W_{12} \gg T_{21}$, the exponential term in Eq. (4) vanishes, and instead we obtain $[g_2/(g_1 + g_2)]N_T$. Equating this saturation limit with Eq. (12), we show that the saturation parameter for the two-level, short-pulse-width model becomes[4,10]

$$(W_{12})^{\mathrm{SAT}} = \frac{g_2}{(g_1 + g_2)\Delta t_{1/2}{}^L}. \tag{13}$$

Hence the laser power at which saturation becomes important increases with decreasing laser-pulse width. The parameter values from Table 1 are used in Eq. (13), which predicts $(W_{12})^{\mathrm{SAT}} = 3.3 \times 10^{10}\ \mathrm{s}^{-1}$. This represents a factor-of-25 increase in the saturation parameter over that defined by the two-level, steady-state model. In previous experiments saturation was observed at an average laser power of 30–40 mW, rather than the expected 850 μW.[3] The additional order-of-magnitude delay could result from the small irradiance that is present in the spatial and the temporal wings of the laser pulse.[4] This effect has been encountered previously in experiments on laser-saturated fluorescence with pulsed lasers.[15] There may be additional causes for the discrepancy between the observed and the predicted saturation parameters,[4] but a detailed discussion of these causes is beyond the scope of the present paper. In our experiments the average laser power is always selected to be less than the laser power that corresponds to the predicted saturation parameter.[6]

For the short pulse widths that are characteristic of mode-locked lasers, further analysis shows that the rate equations for the three-level model reduce to the rate equations that correspond to a two-level model for the transition in resonance.[10] This is true for both the linear and the saturated regimes, although the linear approximation will hold for comparatively longer pulse widths.[10] This conclusion is similar to that for which the balanced cross-rate model holds.[16]

6. Depth of Modulation for Picosecond Pulses

One can analyze the transient absorption induced by a picosecond laser pulse by considering the differential control volume as shown in Fig. 2(a). When a weak pulse passes through the volume, the resulting excited-state population is given by Eq. (12). Be-

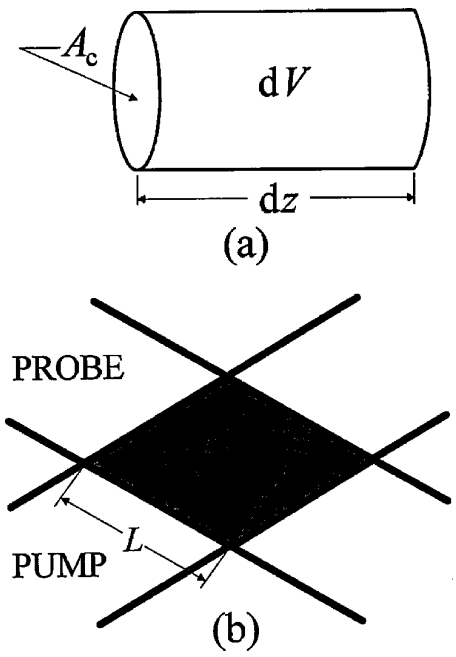

Fig. 2. Geometries used in the calculations: (a) Differential interaction volume for probe absorptance modeling, (b) crossed-beam geometry used for pump–probe absorption modeling.[17]

cause quenching is negligible on the time scale of a single pulse, and stimulated emission is negligible for low laser irradiance, each excited atom that remains after a mode-locked pulse has traversed the control volume must correspond to the loss of one photon from that pulse. The energy of a photon is given by $h\nu_0$; application of an energy balance yields the change in pulse energy per unit volume,

$$\frac{\mathrm{d}E_P{}^L}{\mathrm{d}V} = -h\nu_0 N_T W_{12} \Delta t_{1/2}{}^L. \tag{14}$$

Substituting Eq. (8) for the rate coefficient for stimulated absorption, and applying Eq. (9) with $P_{\mathrm{AVE}}{}^L = f^L E_P{}^L$, we obtain

$$\frac{\mathrm{d}I^L}{I^L} = -\frac{g_2}{g_1} \frac{\ln\left(\frac{1}{\sqrt{2}-1}\right) c^2 A_{21} N_T}{8\pi\nu_0{}^2 \Delta\nu_{1/2}{}^L}\,\mathrm{d}z. \tag{15}$$

Integration yields a Beer–Lambert attenuation expression.[8] Thus, although the use of picosecond pulses substantially changes the form of the rate equations, the absorption expression remains unchanged. Equation (15) is extended to the pump–probe configuration in Section 7.

The pump–probe signal can also be derived in terms of a modulation depth by the use of the absorptance α. The spectral absorptance can be defined as[8,9]

$$\alpha_\nu = \frac{I_\nu{}^L(0) - I_\nu{}^L(L)}{I_\nu{}^L(0)}. \tag{16}$$

If we substitute the spectral form of the Beer–Lambert attenuation equation into Eq. (16), the spectral absorptance becomes[8,9]

$$\alpha_\nu = 1 - \exp\left[-\frac{h\nu_0}{c} B_{12} Y(\nu) N_T L\right]. \tag{17}$$

The total absorptance can be defined as the total absorbed irradiance divided by the total incident irradiance, or

$$\alpha = \frac{\int_{-\infty}^{\infty} \alpha_\nu I_\nu{}^L(0)\,\mathrm{d}\nu}{I^L(0)}. \tag{18}$$

Because the laser linewidth is considerably larger than the linewidth of the medium,[6] we may assume that the laser irradiance is constant at its central value over the spectral profile of the medium. Thus, using Eqs. (7) and (17), we obtain[9]

$$\alpha = \frac{\ln\left(\frac{1}{\sqrt{2}-1}\right)}{\Delta\nu_{1/2}{}^L} \int_{-\infty}^{\infty} \left\{1 - \exp\left[-\frac{h\nu_0}{c} B_{12} Y(\nu) N_T L\right]\right\}\mathrm{d}\nu, \tag{19}$$

where $Y(\nu)$ is given by the Voigt profile.[18,19]

For small optical depths $N_T L$, the optically thin limit can be shown to take the form[9,19]

$$\alpha^{\mathrm{THIN}} = \frac{\ln\left(\frac{1}{\sqrt{2}-1}\right)}{\Delta\nu_{1/2}{}^L} \frac{g_2}{g_1} \frac{c^2 A_{21} N_T L}{8\pi\nu_0{}^2}, \tag{20}$$

whereas for optically thick conditions, the absorptance becomes[9,19]

$$\alpha^{\mathrm{THICK}} = \frac{\ln\left(\frac{1}{\sqrt{2}-1}\right)}{\Delta\nu_{1/2}{}^L} \left[\frac{g_2}{g_1} \frac{c^2 A_{21} (\Delta\nu_{1/2})_c N_T L}{4\pi\nu_0{}^2}\right]^{1/2}. \tag{21}$$

Here $(\Delta\nu_{1/2})_c$ is the collision-broadened linewidth of the resonant transition (s^{-1}). These two limits serve as a convenient means of defining the end of the linear (optically thin) absorption regime; if we define this limit in terms of the optical depth for which $\alpha^{\mathrm{THIN}} = \alpha^{\mathrm{THICK}}$, the critical optical depth becomes

$$N_T L = \frac{g_2}{g_1} \frac{16\pi\nu_0{}^2 (\Delta\nu_{1/2})_c}{c^2 A_{21}}. \tag{22}$$

Using appropriate parameter values from Table 1, we find that the critical optical depth becomes 3.2×10^{11} cm^{-2}. This is the upper limit for which pump–probe measurements can be assumed to be of practical use and is in excellent agreement with our quantitative experimental results.[6]

7. Absorption in the Pump–Probe Configuration

In this section we develop a model that predicts the modulation of a probe laser from a pump-induced population distribution. This model will allow us to make an estimate of the minimum population that can be detected with picosecond pump–probe absorption spectroscopy. The model is then modified to include the ASOPS technique for measuring excited-state lifetimes.

Using the geometry shown in Fig. 2(b),[17] we assume that the pump and the probe beams are cylinders with a diameter equal to the focal diameter. The interaction length L corresponds to one side of the parallelogram formed where the beams cross. For the present calculations the two-level excitation scheme shown in Fig. 1(a) is chosen. Identical pulse widths are assumed for each laser, and both laser repetition frequencies f^L are equal, as was the case for previous pump–probe studies with synchronously mode-locked dye lasers.[5,20]

When a pump pulse passes through the interaction volume, Eq. (12) indicates that the excited-state population becomes $N_2{}^{\text{pump}} = N_T \Delta t_{1/2}{}^L W_{12}$. From Eq. (8) this can be expressed as

$$N_2{}^{\text{pump}} = \frac{g_2}{g_1} \frac{\ln\left(\frac{1}{\sqrt{2}-1}\right) c^2 A_{21} \Delta t_{1/2}{}^L N_T I^{\text{pump}}}{8\pi h \nu_{12}{}^3 \Delta \nu_{1/2}{}^L}. \quad (23)$$

When we substitute Eqs. (9) and (23) into Eq. (20) for optically thin absorptance between levels 2 and 3, the probe modulation, in terms of the average pump-laser power, becomes

$$\alpha_{\text{MOD}} = \frac{g_3}{g_1}\left[\ln\left(\frac{1}{\sqrt{2}-1}\right)\right]^2 \frac{c^4 A_{21} A_{32} P_{\text{AVE}}{}^{\text{pump}} N_T L}{16\pi^3 D^2 h \nu_{12}{}^3 \nu_{23}{}^2 f^L (\Delta \nu_{1/2}{}^L)^2}. \quad (24a)$$

Now suppose that the pump is tuned to the $3S_{1/2}$–$3P_{3/2}$ transition of sodium, while the probe is tuned to the $3P_{3/2}$–$4D_{5/2}$ transition. For this configuration, appropriate spectroscopic constants have been compiled in part (c) of Table 1. Because of the convention of Fig. 1(b), Eq. (24a) must also be modified to take the form

$$\alpha_{\text{MOD}} = \frac{g_4}{g_1}\left[\ln\left(\frac{1}{\sqrt{2}-1}\right)\right]^2 \frac{c^4 A_{31} A_{43} P_{\text{AVE}}{}^{\text{pump}} N_T L}{16\pi^3 D^2 h \nu_{13}{}^3 \nu_{34}{}^2 f^L (\Delta \nu_{1/2}{}^L)^2}. \quad (24b)$$

Using additional parameters from part (b) of Table 1, along with 1 mW of pump-laser power (to preclude saturation), we predict a modulation depth of $(9.8 \times 10^{-14}\ \text{cm}^2)\ N_T L$. For a 2.9° crossing angle,[6] the effective path length becomes 0.15 cm, for which $\alpha_{\text{mod}} = (1.5 \times 10^{-14}\ \text{cm}^3)\ N_T$. For high-frequency modulation, with both the pump and the probe lasers operating at the same repetition frequency, and a 1-s time constant for detection with a lock-in amplifier, a minimum modulation depth of approximately 10^{-8} can be detected.[21] This corresponds to a minimum detectable population of $N_T = 6.8 \times 10^5\ \text{cm}^{-3}$.

A more favorable prediction results if both beams are tuned to coincide with the D_2 line. In this case α_{mod} will have contributions from two sources, which we can conveniently derive by again applying conservation of energy. One contribution is gain from $3P_{3/2}$–$3S_{1/2}$ stimulated emission. This gain in energy per unit volume is given by $h\nu_{12} N_2{}^{\text{pump}} W_{21}{}^{\text{probe}} \Delta t_{1/2}{}^L$, where $N_2{}^{\text{pump}}$ is given by Eq. (23). The other contribution arises from a decrease in ground-state absorption caused by a pump-induced reduction in the ground-state population density. This apparent gain in energy per unit volume can be expressed as $h\nu_{12} N_2{}^{\text{pump}} W_{12}{}^{\text{probe}} \Delta t_{1/2}{}^L$. Summing the contributions to α_{mod}, we write

$$\frac{\mathrm{d}E_p{}^{\text{probe}}}{\mathrm{d}V} = \left(1 + \frac{g_1}{g_2}\right) h\nu_{12} N_2{}^{\text{pump}} \Delta t_{1/2}{}^L W_{12}{}^{\text{probe}}. \quad (25)$$

Thus the detection limit improves because modulation takes place from two processes. Note that for each contribution, α_{mod} will be negative if the convention of Eq. (16) is followed. Kneisler[22] included a discrete variable that could take on a value of ± 1 depending on whether the modulation resulted from stimulated emission or from absorption. No such variable is used here, and the negative sign is dropped in these calculations, although the gain or loss taking place should be noted. Solving the differential equation, and again expressing the result in terms of average pump power, we obtain an optically thin modulation depth of[9]

$$\alpha_{\text{MOD}} = \frac{g_2}{g_1}\left(1 + \frac{g_1}{g_2}\right)\left[\ln\left(\frac{1}{\sqrt{2}-1}\right)\right]^2 \frac{c^4 A_{21}{}^2 P_{\text{AVE}}{}^{\text{pump}} N_T L}{16\pi^3 D^2 h \nu_{12}{}^5 f^L (\Delta \nu_{1/2}{}^L)^2}. \quad (26)$$

Using parameter values from Table 1, along with a 1-mW pump beam crossed at 2.9° with the probe beam, we find a detection limit of $N_T = 6 \times 10^4\ \text{cm}^{-3}$ is found for a modulation depth of 10^{-8}. This value is similar to the experimentally obtained detection limit of $6.5 \times 10^4\ \text{cm}^{-3}$ reported by Langley *et al.*[5] for the $2S_{1/2} - 2P_{1/2,3/2}$ transition of atomic lithium.

The eventual application of pump–probe spectroscopy in a practical measurement scheme would be to detect hydroxyl.[3] For the $Q_1(9)$ line of the $A\ ^2\Sigma^+$ $(v' = 0)$–$X^2\Pi$ $(v'' = 0)$ transition at 2000 K, the inverse Boltzmann fraction is 53.5, the detection frequency ν_0 is $9.7 \times 10^{14}\ \text{s}^{-1}$, and A_{21} is $6.36 \times 10^5\ \text{s}^{-1}$.[17] Using the theory of Section 4, we find that the average power required to saturate this transition with a 20-ps pulse is 900 mW. Thus the maximum available UV power for our laser systems can be used. This value happens to be approximately 1 mW.[23] Using a 1-mW pump power in Eq. (26), we obtain a probe modulation of $\alpha_{\text{mod}} = (1.5 \times 10^{-18}\ \text{cm}^2)\ N_T L$. For an effective interaction path of $L = 0.15$ cm and a modulation depth of 10^{-8}, we estimate a detection

limit of $N_{OH} = 2.3 \times 10^{12}\ cm^{-3}$. This limit is of value to combustion researchers because hydroxyl can be present in flames at concentrations that are several orders of magnitude larger.

8. ASOPS Absorption Model

The pump–probe instrument can also be used to measure excited-state lifetimes by delaying the probe–pulse train relative to the pump-pulse train.[5] In our experiments we vary the delay automatically by the use of the ASOPS technique.[3,6] In this case additional theory must be included to account for the presence of temporal decays.

After excitation by a pump pulse, the excited-state population is again given by Eq. (23). In the absence of a probe pulse this population will decay exponentially following Eq. (1), at a rate governed by

$$N_2(t) = N_2{}^{\text{pump}} \exp[-(Q + A)t]. \tag{27}$$

If we assume that the pump–probe configuration follows Fig. 1(a), Eq. (24a) yields a probe-beam modulation of

$$\alpha_{\text{MOD}}(t) = \frac{g_3}{g_1}\left[\ln\left(\frac{1}{\sqrt{2}-1}\right)\right]^2 \frac{c^4 A_{21} A_{32} \Delta t_{1/2}{}^L I^{\text{pump}} N_T L}{64\pi^2 h \nu_{12}{}^3 \nu_{23}{}^2 (\Delta \nu_{1/2}{}^L)^2} \times \exp[-(Q + A)t], \tag{28}$$

where we have converted to the pump irradiance with Eq. (9). The overall detection efficiency η_d in volts per cubic centimeter per watt is introduced to account for the optical and the electronic detection characteristics. Noting that the photodetector output will be proportional to the amount of absorbed light at the modulation frequency, we can write the instantaneous ASOPS signal (V) as

$$S(t) = \eta_d I^{\text{probe}} \alpha_{\text{MOD}}(t). \tag{29}$$

Substituting $\alpha_{\text{MOD}}(\pm)$ from Eq. (28) and converting irradiance back to average power, we find that the pump–probe model for a two-level absorber yields

$$S(t) = \eta_d \frac{g_3}{g_1}\left[\ln\left(\frac{1}{\sqrt{2}-1}\right)\right]^2 \times \frac{c^2 A_{21} A_{32} P_{\text{AVE}}{}^{\text{pump}} P_{\text{AVE}}{}^{\text{probe}} N_T L}{4\pi^4 D^4 h \nu_{12}{}^3 \nu_{23}{}^2 f^{\text{pump}} f^{\text{probe}} \Delta t_{1/2}{}^L (\Delta \nu_{1/2}{}^L)^2} \times \exp[-(Q + A)t]. \tag{30}$$

The linear dependence of the ASOPS signal on the pump-beam and the probe-beam power has been experimentally verified for atomic sodium excitation in an atmospheric-pressure hydrocarbon flame.[3] A curve fit to Eq. (30) will yield Q, which can be used to correct for the effects of quenching, allowing us to obtain quantitative results.

9. Dual-Beam ASOPS

The simplicity of the quenching-correction scheme is lost when a multilevel atom or molecule is detected.[3] A prime example is atomic sodium, for which level 2 must be split into two individual components to account for the presence of the $3P$ doublet. Levels 1, 2, and 3 correspond to the $3S_{1/2}$, $3P_{1/2}$, and $3P_{3/2}$ states, respectively. The pump beam resonantly excites either the $3S_{1/2}$–$3P_{1/2}$ transition or the $3S_{1/2}$–$3P_{3/2}$ transition. The probe beam is, in this example, permitted to connect either the $3P_{1/2}$ or the $3P_{3/2}$ level to a level of higher energy, such as the $5S_{1/2}$ or the $4D_{3/2,5/2}$ levels. The unfortunate consequence of the $3P$ doublet is the introduction of a second unknown collisional parameter, the doublet mixing-rate coefficient.

As an example consider the case in which both beams are tuned to the D_2 transition. The ASOPS signal is then the sum of two contributions. The first contribution is due to stimulated emission by the probe, which is given by $h\nu_{13} N_3(t) \Delta t_{1/2}{}^L W_{31}{}^{\text{probe}}$. The second contribution, resulting from apparent gain, is given by $h\nu_{13} N_3(t) \Delta t_{1/2}{}^L W_{13}{}^{\text{probe}}$. Summing the two terms gives us the expression

$$\frac{dE_p{}^{\text{probe}}}{dV} = h\nu_{13} N_3(t) \Delta t_{1/2}{}^L (W_{13}{}^{\text{probe}} + W_{31}{}^{\text{probe}}). \tag{31}$$

Substituting **what** for $N_3(t)$ from Eq. (6), we find that the overall energy balance becomes

$$\frac{dE_p{}^{\text{probe}}}{dV} = \frac{2}{3}\left(1 + \frac{g_1}{g_3}\right) h\nu_{13} \Delta t_{1/2}{}^L W_{13}{}^{\text{probe}} N_3{}^{\text{pump}} \times \left\{\exp[-(Q + A)t] + \frac{1}{2}\exp[-(Q + A + 3Q_{32})t]\right\}. \tag{32}$$

Substituting $W_{13}{}^{\text{probe}}$ from Eqs. (8) and (9), we can convert the energy balance to an expression in terms of average laser power. When we integrate and convert Eq. (32) to a modulation depth, the corresponding temporal ASOPS signal then becomes[9,20]

$$S(t) = \frac{2}{3}\eta_d \frac{g_3}{g_1}\left(1 + \frac{g_3}{g_1}\right) \frac{c^4 A_{31}{}^2 P_{\text{AVE}}{}^{\text{pump}} P_{\text{AVE}}{}^{\text{probe}} N_T L[\exp[-(Q + A)t] + \tfrac{1}{2}\exp[-(Q + A + 3Q_{32})t]]}{\left[\ln\left(\frac{1}{\sqrt{2}-1}\right)\right]^{-2} 4\pi^4 D^4 h \nu_{13}{}^5 f^{\text{pump}} f^{\text{probe}} \Delta t_{1/2}{}^L (\Delta \nu_{1/2}{}^L)^2}. \tag{33}$$

Equation (33) contains three unknowns (N_T, Q, and Q_{32}). Fiechtner *et al.*[3] fitted their ASOPS decay by assuming a value from the literature for the ratio Q/Q_{32}. The value of this ratio will not always be known. Clearly a better method is needed for lifetime measurements.

Consider the case in which the pump is tuned to the D_1 line, while the probe is tuned to the D_2 line. When the respective contributions from stimulated emission and apparent gain are summed, an energy balance yields

$$\frac{\mathrm{d}E_p^{\text{probe}}}{\mathrm{d}V} = h\nu_{13}\Delta t_{1/2}{}^{L}\left[N_3(t)W_{31}{}^{\text{probe}} + N_2(t)W_{13}{}^{\text{probe}}\right]. \tag{34}$$

Following the above procedures, we can show that the corresponding ASOPS signal takes the form[9,20]

$$S(t) = \frac{2}{3}\eta_d \frac{c^4 A_{31}A_{21}P_{\text{AVE}}{}^{\text{pump}}P_{\text{AVE}}{}^{\text{probe}}N_T L\{2\exp[-(Q+A)t] + \exp[-(Q+A+3Q_{32})t]\}}{\left[\ln\left(\frac{1}{\sqrt{2}-1}\right)\right]^{-2} 4\pi^4 D^4 h\nu_{12}{}^3\nu_{13}{}^2 f^{\text{pump}} f^{\text{probe}}\Delta t_{1/2}{}^{L}(\Delta\nu_{1/2}{}^{L})^2}, \tag{35}$$

where $g_1 = g_2 = 2$ and $g_3 = 4$ have been applied. Equation (35) contains the same two unknown collisional parameters. However, for this particular pump–probe configuration, both beams are modulated.[6] Because the D_1 beam excites a different transition, the corresponding decay will be governed by an equation that differs from Eq. (35). By simultaneously detecting both beams, we can determine both Q and Q_{32} with a single measurement. In this case both beams serve as the pump and the probe. This method, which we call the dual-beam ASOPS method, has been experimentally demonstrated by our research group.[6]

We can derive the signal on the D_1 beam by again summing the contributions from stimulated emission and apparent gain to obtain

$$\frac{\mathrm{d}E_p^{\text{probe}}}{\mathrm{d}V} = h\nu_{12}\Delta t_{1/2}{}^{L}\left[N_2(t)W_{21}{}^{\text{probe}} + N_3(t)W_{12}{}^{\text{probe}}\right]. \tag{36}$$

The corresponding ASOPS signal becomes[9]

$$S(t) = \eta_d\left[\ln\left(\frac{1}{\sqrt{2}-1}\right)\right]^2 \times \frac{c^4 A_{21}A_{31}P_{\text{AVE}}{}^{\text{pump}}P_{\text{AVE}}{}^{\text{probe}}N_T L}{4\pi^4 D^4 h\nu_{12}{}^2\nu_{13}{}^3 f^{\text{pump}} f^{\text{probe}}\Delta t_{1/2}{}^{L}(\Delta\nu_{1/2}{}^{L})^2} \times \exp[-(Q+A)t]. \tag{37}$$

The simple exponential decay results from the equal degeneracies of the levels that are connected by the probe. Because Eq. (37) predicts an exponential decay in terms of only Q, the corresponding excitation scheme is used frequently in our experiments.[6] This fortunate result may not be possible when one is detecting species other than sodium with dual-beam ASOPS. Nevertheless both Q and Q_{32} can still be obtained from a single measurement, in contrast to previous ASOPS studies.[3]

10. Coherent Transient Interferences

Quenching-independent concentration measurements are possible when $\Delta t_{1/2}{}^{L} \ll Q_{21}{}^{-1}$. However, this methodology can also lead to the presence of coherent transients. When coherent transients are important, theory must be developed with the density matrix equations. Nevertheless the use of rate equations is justified if the coherence time of the laser is short compared with the pumping time.[24] The coherence time is the reciprocal of the bandwidth,[25] and the pumping time is the reciprocal of the absorption probability.[24] Thus the present pump–probe model should hold if $W_{12} \ll \Delta\nu_{1/2}{}^{L}$.

For our bandwidth of 1.6×10^{10} s^{-1} and the parameter values given in part (c) of Table 1, we estimate that an average laser power of less than 420 μW is required for avoidance of coherent transients. This could explain the negative artifact that we observed in previous ASOPS experiments, in which the laser power was greater than 10 mW.[12] In this case the artifact was probably caused by perturbed free induction decay.[20] For cases in which the above inequality is only moderately violated, coherent transient effects may not be important. The spatial profile of the laser requires that the interaction between the laser and the atoms be averaged over different irradiances.[24] Moreover we estimate the value applied for $\Delta\nu_{1/2}{}^{L}$ by assuming that the laser pulses are transform limited. Our laser pulses are not perfectly transform limited, and thus the bandwidth of 1.6×10^{10} s^{-1} represents a minimum value. In our present experiments[6] we use a 700-μW average power and find that we can obtain ASOPS signals for which the magnitude of coherent effects is negligible.

11. Conclusions

A model has been developed to predict practical operating limits when one is using synchronously mode-locked dye lasers for picosecond pump–probe absorption spectroscopy. The model agrees closely with several experimental observations. The prediction of the optically thick limit is nearly the same as our experimentally observed value.[6] The minimum detectability corresponding to the shot-noise limit is estimated, and the resulting prediction corresponds

well with the experimentally observed detection limit of Jones and coworkers.[5] The pump–probe model has also been modified to include the problem of measuring excited-state lifetimes. For a three-level absorber such as atomic sodium, a new technique that permits measurement of the excited state lifetime in a single measurement is proposed. This is in contrast to our previous experiments with atomic sodium with the ASOPS method,[3] in which a single measurement would not directly yield an estimate for Q. We call the new technique dual-beam ASOPS. We report the successful demonstration of dual-beam ASOPS in a companion paper.[6]

Based on the agreement of the model with experiments, we have chosen to apply it in calculations concerning future measurements of minor flame species. In particular, for a 1-s integration time, we predict a detection limit for hydroxyl of 2.3×10^{12} cm^{-3}. Unfortunately the detection of hydroxyl is complicated by the low average power that our laser systems produce in the UV. Some improvements are suggested in the companion paper.[6]

The authors are extremely grateful for the advice of Fred Lytle, Department of Chemistry, Purdue University. We also thank Campbell D. Carter, Systems Research Laboratories, Inc. (a division of Arvin/Calspan), Dayton, Ohio, and John R. Reisel, School of Mechanical Engineering, Purdue University, for their helpful discussions concerning OH spectroscopy. This work was sponsored by the U.S. Air Force Office of Scientific Research, U.S. Air Force Systems Command, under grant AFOSR-89-0051.

References

1. A. C. Eckbreth, *Laser Diagnostics for Combustion Temperature and Species* (Abacus, Cambridge, Mass., 1988).
2. R. P. Lucht, "Applications of laser-induced fluorescence spectroscopy for combustion and plasma diagnostics," in *Laser Spectroscopy and Its Applications*, L. J. Radziemski, R. W. Solarz, and J. A. Paisner, eds. (Dekker, New York, 1987), pp. 623–676.
3. G. J. Fiechtner, G. B. King, N. M. Laurendeau, and F. E. Lytle, "Measurements of atomic sodium in flames by asynchronous optical sampling: theory and experiment," Appl. Opt. **31,** 2849–2864 (1992).
4. C. Th. J. Alkemade, "Anomalous saturation curves in laser-induced fluorescence," Spectrochim. Acta Part B, **40,** 1331–1368 (1985).
5. A. J. Langley, R. A. Beaman, J. Baran, A. N. Davies, and W. J. Jones, "Concentration-modulated absorption spectroscopy," Opt. Lett. **10,** 327–329 (1985); A. J. Langley, R. A. Beaman, A. N. Davies, W. J. Jones, and J. Baran, "Concentration-modulated absorption spectroscopy I," Chem. Phys. **101,** 117–125 (1986); R. A. Beaman, A. N. Davies, A. J. Langley, W. J. Jones and J. Baran, "Concentration-modulated absorption spectroscopy: II. Temporal variation of gain," Chem. Phys. **101,** 127–132 (1986).
6. G. J. Fiechtner, G. B. King, and N. M. Laurendeau, "Quantitative concentration measurements of atomic sodium in an atmospheric hydrocarbon flame with asynchronous optical sampling (ASOPS)," Appl. Opt. **33,** 1117–1126 (1994).
7. R. P. Lucht and N. M. Laurendeau, "Comment on 'laser-induced fluorescence measurement of sodium in flames,'" Combust. Flame **34,** 215–217 (1979).
8. R. M. Measures, *Laser Remote Sensing* (Wiley, New York, 1984).
9. G. J. Fiechtner, "Quantitative concentration measurements in atmospheric-pressure flames by picosecond pump/probe absorption spectroscopy," Ph.D. dissertation (Purdue University, West Lafayette, Ind., 1992).
10. Y. Takubo, T. Okamoto, and M. Yamamoto, "Laser spectroscopic measurement of quenching and doublet mixing rates of the Na ($3P_{3/2,1/2}$) doublet in a propane–air flame," Appl. Opt. **25,** 740–743 (1986).
11. G. J. Blanchard and M. J. Wirth, "Transform-limited behavior from the synchronously pumped cw dye laser," Opt. Commun. **53,** 394–400 (1985).
12. G. J. Fiechtner, Y. Jiang, G. B. King, N. M. Laurendeau, R. J. Kneisler, and F. E. Lytle, "Determination of relative number density and decay rate for atomic sodium in an atmospheric premixed flame by asynchronous optical sampling," in *Twenty-Second Symposium (International) on Combustion* (Combustion Institute, Pittsburgh, Pa., 1988), pp. 1915–1921.
13. N. Omenetto, "Response time of two- and three-level atomic and molecular systems to steplike excitation," Spectrochim. Acta Part B **37,** 1009–1014 (1982).
14. D. Stepowski and M. J. Cottereau, "Direct measurement of OH local concentration in a flame from the fluorescence induced by a single laser pulse," Appl. Opt. **18,** 354–356 (1979).
15. J. T. Salmon and N. M. Laurendeau, "Analysis of probe volume effects associated with laser-saturated fluorescence measurements," Appl. Opt. **24,** 1313–1321 (1985).
16. R. P. Lucht, D. W. Sweeney, and N. M. Laurendeau, "Balanced cross-rate model for saturated fluorescence in flames using a nanosecond pulse length laser," Appl. Opt. **19,** 3295–3300 (1980).
17. G. J. Blanchard and M. J. Wirth, "Measurement of small absorbances by picosecond pump–probe spectrometry," Anal. Chem. **58,** 532–535 (1986).
18. R. P. Lucht, R. C. Peterson, and N. M. Laurendeau, "Fundamentals of absorption spectroscopy for selected diatomic flame radicals," PURDU-CL-78-06 (Purdue University, West Lafayette, Ind., 1978).
19. A. C. G. Mitchell and M. W. Zemansky, *Resonance Radiation and Excited Atoms* (Cambridge U. Press, London, 1961).
20. B. A. Mann, "Novel coherent laser spectroscopic techniques for minor species combustion diagnostics," Ph.D. dissertation (University of Reading, Whiteknights, Reading, Berks., England, 1991).
21. J. P. Heritage, "Picosecond nonlinear spectroscopy of silver microstructures and surface adsorbates," in *Advances in Laser Spectroscopy 2*, B. A. Garetz and J. R. Lombardi, eds. (Wiley, New York, 1983), pp. 207–224.
22. R. J. Kneisler, "Construction and development of a picosecond UV pump/UV probe spectrometer for combustion diagnostics based on asynchronous optical sampling (ASOPS)," Ph.D. dissertation (Purdue University, West Lafayette, Ind., 1990).
23. G. J. Fiechtner, G. B. King, N. M. Laurendeau, R. J. Kneisler, and F. E. Lytle, "Efficient frequency doubling for synchronously mode-locked dye lasers," Appl. Spectrosc. **43,** 1286–1287 (1989).
24. R. Altkorn and R. N. Zare, "Effects of saturation on laser-induced fluorescence measurements of population and polarization," Ann. Rev. Phys. Chem. **35,** 265–289 (1984).
25. P. Avan and C. Cohen-Tannoudji, "Two-level atom saturated by a fluctuating resonant laser beam: calculation of the fluorescence spectrum," J. Phys. B **10,** 155–170 (1977).